

# THE HIDDEN BLOAT IN MACHINE LEARNING SYSTEMS

Huaifeng Zhang<sup>1</sup> Ahmed Ali-Eldin<sup>1</sup>

## ABSTRACT

Software bloat refers to code and features that is not used by a software during runtime. For Machine Learning (ML) systems, bloat is a major contributor to their technical debt leading to decreased performance and resource wastage.

In this work, we present, *Negativa-ML*, a novel tool to identify and remove bloat in ML frameworks by analyzing their shared libraries. Our approach includes novel techniques to detect and locate unnecessary code within device code - a key area overlooked by existing research, which focuses primarily on host code. We evaluate *Negativa-ML* using four popular ML frameworks across ten workloads over 300 shared libraries. The results demonstrate that the ML frameworks are highly bloated on both the device and host code side. On average, *Negativa-ML* reduces the device code size in these frameworks by up to 75% and the host code by up to 72%, resulting in total file size reductions of up to 55%. The device code is a primary source of bloat within ML frameworks. Through debloating, we achieve reductions in peak host memory usage, peak GPU memory usage, and execution time by up to 74.6%, 69.6%, and 44.6%, respectively.

## 1 INTRODUCTION

Machine learning (ML) has affected many industries significantly. From personalized recommendations (Ko et al., 2022), to healthcare diagnostics (Bhardwaj et al., 2017), and autonomous vehicles (Parekh et al., 2022), ML is revolutionizing nearly every sector. Not only Large Language Models (LLMs) that enabled natural language understanding and content generation like ChatGPT (OpenAI et al., 2024) and Llama (Touvron et al., 2023b) have propelled this transformation, but also smaller models that are now widely deployed in many vision applications from cameras to mobile phones. However, as these models grow in numbers, size, and complexity, managing and optimizing ML systems has become increasingly challenging. LLMs often contain billions of parameters, requiring substantial computational resources and vast amounts of training data. Some smaller models are now deployed on embedded devices. To manage this complexity, substantial technical overhead is introduced to ML systems, exacerbating the issue of software bloat within these systems (Zhang et al., 2024).

Software bloat refers to code that is unnecessary for a program during runtime, typically caused by extraneous functions, libraries, or features that do not contribute to the core

functionality. Software bloat can cause a range of issues, including decreased performance, increased resource usage, and security vulnerabilities. While bloat can affect any type of software, ML systems have a special capacity for incurring it, because they have all the maintenance problems of traditional code plus an additional set of ML-specific issues, such as boundary erosion, data dependencies, etc. (Sculley et al., 2015). As ML models grow in scale and complexity, the bloat in ML systems compounds, leading to further inefficiencies that hinder runtime performance and increase the cost of deployment, particularly in resource-constrained environments (Zhang et al., 2024; Jiang et al., 2020).

At the heart of ML systems are ML frameworks, such as TensorFlow (Abadi et al., 2016) and PyTorch (Paszke et al., 2019). These frameworks provide the essential libraries and tools for model training and inference. ML frameworks are typically developed using multiple programming languages with C++ and CUDA used to implement the core functionalities, focusing on maximizing performance. Both C++ and CUDA code are compiled into shared libraries. Python acts as the frontend, wrapping these core functionalities and enhancing the frameworks' usability for developers. However, with the ease of use and flexibility that these frameworks provide, they also introduce *framework tax* (Fernandez et al., 2023) - these frameworks can introduce performance overheads and diminish the benefits of new hardware and model architecture advancements. Furthermore, integrating these frameworks also leads to large binary sizes and brings unnecessary overhead for mobile and edge devices (Jiang et al., 2020).

<sup>1</sup>Chalmers University of Technology, Sweden. Correspondence to: Huaifeng Zhang <huaifeng@chalmers.se>, Ahmed Ali-Eldin <ahmed.hassan@chalmers.se>.

In this paper, we aim to identify and reduce bloat in ML frameworks, targeting the bloat in ML shared libraries. These shared libraries encapsulate the core functionalities of ML frameworks and constitute the majority of ML framework size. Debloating ML shared libraries involves the following challenges:

- ML frameworks rely on some proprietary libraries, such as cuDNN (nvi, b) and cuBLAS (nvi, c). These libraries are not open-sourced, making it impossible to perform source code analysis.
- ML frameworks contain code that runs on both the host (CPU) and device (GPU). Device code is overlooked by existing research and no method measure and reduce bloat in it.
- Although host code has a well-defined structure and the bloat in it has been previously studied (anonymous), the structure of device code is not publicly available, making it difficult to analyze and debloat.

To address these challenges, we propose a tool, *Negativa-ML*, to identify and remove bloat in both host and device code within ML shared libraries. Leveraging insights into how ML systems execute ML workloads on host and device, we propose a novel approach to detect the device code used by an ML workload with low performance overhead. Subsequently, we locate the file ranges occupied by this device code within ML shared libraries. This involves a deep understanding of how device code is compiled and how they are organized within a shared library, which is challenging because device code structure lacks a public specification. Finally, we utilize a debloating tool that we have previously developed (anonymous) to remove bloat from ML shared libraries according to the file ranges located. Our contributions are as follows:

- We propose an approach to detect device code used by ML workloads with low performance overhead.
- We analyze the structure of device code in ML shared libraries and propose a method to locate the file ranges of used device code.
- We extend a debloating tool that we have developed (anonymous) to remove bloat in both host and device code in ML shared libraries.
- We evaluate *Negativa-ML* on four ML frameworks across ten ML workloads with three models and over 300 shared libraries and perform in-depth analysis of the results. Our evaluation shows the extent of bloat in ML frameworks, their causes and the overhead the bloat incurs.

To the best of our knowledge, this is the first work to evaluate and remove bloat in device code. Our evaluation shows that ML frameworks are highly bloated, with 72% of host code and 75% of device code being unnecessary for target ML workloads. Besides, 10% shared libraries account for up to 90% of the total bloat in the ML frameworks. This bloat not only increases storage overhead but also degrades runtime performance with increased host memory usage, GPU memory usage, and longer execution times.

## 2 BACKGROUND AND RELATED WORK

This section provides background about ML frameworks, ML shared libraries, software bloat and debloating.

### 2.1 ML Frameworks

ML frameworks are software libraries that provide essential tools for building, training, and deploying ML models. Some ML frameworks are general-purpose and designed to support both training and inference for a wide variety of ML models. While others are optimized for specific use cases, such as LLM inference. Two of the most popular general-purpose ML frameworks are TensorFlow (Abadi et al., 2016) and PyTorch (Paszke et al., 2019), both of which are widely adopted in industry and academia. Although the two frameworks target various ML models,

the rise of LLMs has introduced new requirements for ML frameworks, such as efficient KV cache management (Kwon et al., 2023; Sinha et al., 2024). LLM inference — which is highly latency-sensitive and resource-demanding — is particularly challenging. To meet these demands, new frameworks specifically designed for LLM inference have been proposed (Contributors, 2023; Kwon et al., 2023; Wolf et al., 2020; hug).

The core functionalities of ML frameworks are packaged as shared libraries. A shared library is a file that contains machine code that can be shared among different programs. Shared libraries account for the majority of the total size of ML frameworks. For example, in PyTorch and TensorFlow, shared libraries constitute 93% and 75% of the total framework size, respectively.

The standard file format for shared libraries is the Executable and Linkable Format (ELF) (ora), which organizes a file into various sections, such as `.text` and `.data`. A generic shared library only contains code running on CPU in the `.text` section. This CPU-running code is called *host code*. However, ML shared libraries are unique in that they also contain the code designed to run on GPUs, which is referred to as *device code*. This device code is usually included in another section called `.nv_fatbin` in an ML shared library.

Device code significantly increases the size of ML shared libraries compared to traditional ones. The core shared library in PyTorch, `torch.so`, is 881 MB for the GPU version and 482 MB for the CPU version, nearly double the size. Furthermore, device code makes up a substantial portion of these libraries. Analyzing the top four largest shared libraries in PyTorch, device code accounts for between 68% to more than 91% of the size of each shared library, as shown in Figure 1. In contrast, host code represents only a small fraction of these libraries. Despite device code forming the majority of ML shared libraries, no existing research has investigated bloat within device code.

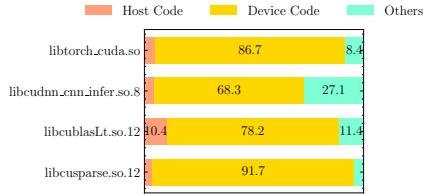


Figure 1. Distribution of host code and device code in the top 4 largest shared libraries in PyTorch.

## 2.2 Software Bloat

Software bloat is mainly caused by unnecessary code in a software, which can be categorized into two types (Brown et al., 2024): Type I bloat is universally unnecessary, for example, dead and unreachable code. Type II bloat is end-use dependent, code may be or may not be Type II bloat depending on the use case, for example, unnecessary program features. Software bloat exists across all the modern software stack, from operating systems (Quach et al., 2017; Kuo et al., 2020), shared libraries (Ziegler et al., 2019; Quach et al., 2018; Biswas et al., 2021), to executables (Navas & Gehani, 2023; Ahmad et al., 2021; Qian et al., 2019) and even containerized applications (Rastogi et al., 2017; Zhang et al., 2024). Bloat causes software to grow in size and complexity over time, which leads to performance degradation, increased memory consumption, longer startup time, and security vulnerabilities, but without providing any additional benefits.

Recently, bloat in ML systems has attracted increasing attention. Sculley et al. (Sculley et al., 2015) identify that ML systems are easy to accumulate hidden technical debt due to a set of ML-specific issues. Zhang et al. (Zhang et al., 2024) show that containerized ML applications are significantly bloated, wasting storage resources and network bandwidth, increasing their attack surface, and slowing down their deployment process.

## 2.3 Software Debloating

Software debloating is the process of removing unnecessary code from software to improve efficiency and reduce

resource consumption. Many debloating tools have been developed for traditional software, which can be categorized by their debloating targets: source code, binary code, and containerized applications. Source code debloating tools eliminate unused code directly from the source, such as dead or unreachable code, based on specific usage scenarios (Brown & Pande, 2019; Ye et al., 2021; Azad et al., 2019). Binary debloating tools operate on software binaries, including shared libraries and executables, to remove unnecessary functions or instructions (Qian et al., 2019; Ahmad et al., 2021; Ziegler et al., 2019; Agadacos et al., 2019). Container debloating tools target containerized applications, removing unnecessary files in container images (Rastogi et al., 2017; Zhang et al., 2023). Most of these tools remove code that is not used by the specific workload, i.e., Type II bloat (Qian et al., 2019; Ahmad et al., 2021; Brown & Pande, 2019; Rastogi et al., 2017; Azad et al., 2019). While debloating traditional software has been extensively studied, to the best of our knowledge, all existing work focus only on traditional applications where code runs only on CPUs. Device code, which constitutes a significant portion of ML frameworks, remains unexamined.

One major issue with debloating tools that focus on binary debloating is that they are generally unreliable (Brown et al., 2024). To solve their reliability issues, we have recently developed *Negativa*, a debloating tool that only debloat host code (anonymous).<sup>1</sup> *Negativa* demonstrates effectiveness in debloating shared libraries, profiling workloads with the target shared libraries, then removing any code not used by the workload. *Negativa*’s debloating process involves three phases: detection, location, and compaction. In the detection phase, it identifies host functions used by the workload; in the location phase, it locates the used host functions within the shared library; and in the compaction phase, it removes unused functions from the shared library and only keeps the used ones.

In this work, we introduce *Negativa-ML*, a technique that we have developed within *Negativa* to enable device code debloating. In addition, we build on *Negativa*’s capabilities to also debloat host code in ML shared libraries. Building on *Negativa*’s three-phase debloating process, we introduce novel approaches for detecting and locating used device code in the detection and location phases. *Negativa*’s compaction phase is then reused to remove unused device code.

## 3 CONVENTION

For the clarity and consistency of the paper, we define the following terms: *Host* refers to CPU and its memory; *Host code* refers to the code that runs on the host; *Functions* specifically refer to the functions in host code. *Device* refers

<sup>1</sup>Please see the supplementary material for details of this tool.

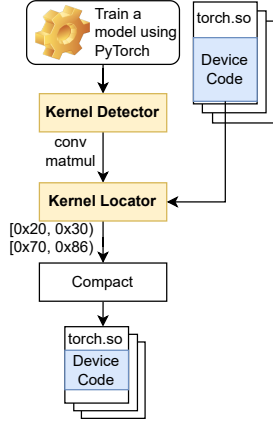


Figure 2. Overview of Negativa-ML. The components proposed in this work are highlighted in yellow rectangles.

to NVIDIA GPUs running on CUDA drivers and its memory; *Device code* refers to the code that runs on the device; *Kernels* refer to the functions in device code.

## 4 METHODOLOGY

Figure 2 provides an overview of Negativa-ML. Negativa-ML is composed of two components: the kernel detector and the kernel locator. During the execution of an ML workload, such as model training with PyTorch, many shared libraries of ML frameworks are utilized. The kernel detector monitors the kernel execution of the workload and records the names of the kernels used. The kernel locator analyzes the shared libraries, extracting device code within these libraries and finding the file ranges of the used kernels within the shared library. These ranges are subsequently passed to Negativa’s compaction module for debloating. Finally, a debloated ML shared library with reduced host code and device code is generated.

### 4.1 Kernel Detector

The kernel detector is responsible for detecting the kernels used by the ML workload. While existing tools like Nsight Systems (NSys) (nvi, f) can profile device code, they are designed primarily for profiling and debugging rather than for used kernel detection. These tools, to provide comprehensive information, usually impose a high performance overhead on the target applications by recording data each time a kernel is called. However, for kernel detection, we are only interested in determining whether a kernel has been used, without needing repetitive call data, which results in unnecessary overhead. To offer a more efficient solution, we propose a novel, lightweight approach that specifically detects kernels used within ML shared libraries, achieving low performance overhead. Since kernels execute on GPU devices, an intuitive approach would be to monitor GPU

device execution directly. However, this approach is not feasible because the code execution on GPU devices is not directly accessible.

Our approach leverages insights into how ML systems execute ML workloads on both the host and the device; Considering the interaction between host and devices, first, the host launches a kernel(s), then the *host-launching kernel* may or maybe not launch other kernels. A kernel launched from another kernel is called *device-launching kernel*. These kernels form a *kernel call graph*, where the start of the graph is the host-launching kernel. The kernel detector only detects host-launching kernels. By monitoring the host code, we can identify kernels launched from the host and subsequently consider them as “used”. This allows us to detect used kernels without the need for GPU-level monitoring.

To launch a kernel from the host, the CUDA driver must call the host function `cuModuleGetFunction` first. The function takes the name of the kernel to be launched as one of its inputs. It returns a function handle, which is used to execute the kernel. Moreover, `cuModuleGetFunction` is only called once for each kernel, no matter how many times the kernel is executed, making it ideally suited for our used kernel detection. Inspired by this observation, we implement a hook to the `cuModuleGetFunction` using Nvidia CUPTI API (nvi, d). This hook records the kernel names passed to the function, which are then considered as used kernels. The kernel detector intercepts each host-launching kernel only once and does not intercept device-launching kernels. Consequently, the performance overhead is lower than profiling tools like NSys.

Figure 3 illustrates an example of the kernel detector workflow. When an ML workload invokes the `matmul` kernel, it first calls the `cuModuleGetFunction`, which resides in the host code, to launch the kernel. The kernel detector intercepts the call to `cuModuleGetFunction` and records the kernel name, marked as a used kernel, which is `matmul` in this example. This kernel may launch other kernels in the device code and form a kernel call graph. However, these device-launching kernels are not detected by the kernel detector.

The kernel detector outputs a list of names of host-launching kernels. These kernels are considered as used kernels and are passed to the kernel locator for further processing. Device-launching kernels are also handled by the kernel locator, as we show in the next section.

### 4.2 Kernel Locator

The kernel locator locates the file ranges (start and end file offset) of the used kernels in the ML shared library. It identifies a list of file ranges that need to be retained in the shared library. The difficulty in locating kernels in the



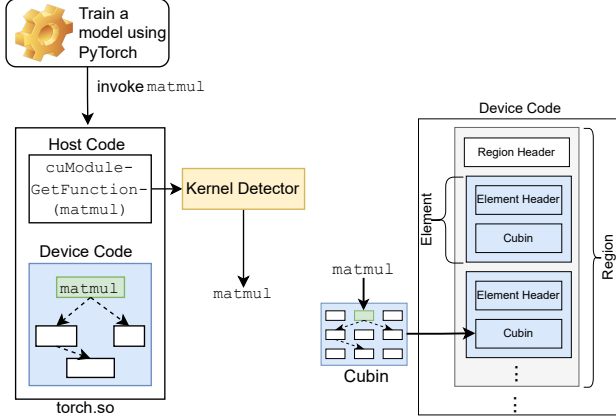


Figure 3. Kernel detector work-flow. Figure 4. Structure of device code.

device code is that there is no public specification for the structure of the device code. Finding the exact location of used kernels requires in-depth reverse engineering of the device code, which can be overfitted to a specific version of the CUDA toolkit and error-prone. In addition, because device-launching kernels are not detected by the kernel detector, the kernel locator must also handle these kernels appropriately to avoid mistakenly removing them.

To address these issues, we propose an approach to *approximately* locate the used kernels in the device code. Instead of finding the exact location of kernels, we find the location of the *cubins* that contain the kernels. A cubin is a CUDA binary file that contains kernel code. If a kernel is launched by another kernel, the two kernels are compiled into the same cubin (nvi, e). Based on this observation, we can deduce that if a cubin contains a host-launching kernel, it also contains all the kernels in the kernel call graph starting from the host-launching kernel, including those device-launching kernels. Therefore, retaining a cubin that contains a host-launching kernel also retains all the kernels in the kernel call graph starting from the host-launching kernel, including those device-launching kernels as well.

To find whether a cubin contains a host-launching kernel, we use the `cuobjdump` tool (nvi, a) to extract a list of cubin files from the shared library. For each cubin, we extract the kernels included in it using `cuobjdump`. If a cubin contains a used host-launching kernel, the whole cubin needs to be retained. In doing so, we also retain the device-launching kernels in the cubin. The next step is to locate the cubin in the shared library file, i.e., find the file range occupied by the cubin. This involves understanding the structure of the device code in the shared library. As shown in Figure 4, the device code in a shared library is organized as a list of *regions*. Each region includes a region header and a list of *elements*. Each element includes an element header and a cubin. A cubin extracted by `cuobjdump`

has an index starting from 1 in its file name. This index is equal to the index of the element containing the cubin in the shared library. Using this index, we can map the cubin to the corresponding element in the shared library. In doing so, we can locate the file range occupied by the cubin.

To maintain the integrity of the shared library, the kernel locator retains or removes the whole element containing a cubin. Finally, the kernel locator uses the following criteria to determine whether to retain an element; The element header has a field called *compute-capability*, which shows the GPU architecture the cubin is compiled for. We find that only the elements that match the GPU architecture can be loaded into the GPU memory. Therefore, if an element matches the GPU architecture which the ML workload is running on *and* contains a cubin that has used host-launching kernels, then we retain the element.

Figure 4 also shows an example of the relationship between kernels, cubins and elements in the shared library. The used kernel `matmul`, which is detected by the kernel detector, is contained in a cubin as shown in the figure. The kernel may launch other kernels, forming a kernel call graph. All the kernels in the kernel call graph are contained in the same cubin. The cubin is in turn contained in an element in the shared library. By retaining the whole element, we ensure that all the kernels in the kernel call graph are retained, including the device-launching kernels in the call graph.

**Compaction:** The file ranges occupied by elements that meet the criteria are retained in the ML shared library, while the rest are removed. This process is handled by Negativa’s compaction phase. In this phase, the unused files are zeroed out. Negativa then maps the file offsets to their original memory addresses where the original shared library is loaded into memory to retain memory address validity. More details on the compaction process can be found in our supplementary material.

## 5 EXPERIMENTS

We evaluate Negativa-ML’s bloat removal with four ML frameworks: two general-purpose ML frameworks, PyTorch and TensorFlow for their wide usage; and two LLM inference frameworks, vLLM (Kwon et al., 2023) and Transformers (Wolf et al., 2020) for their state-of-the-art performance. Using these frameworks, we run various ML workloads with both training or inference of different popular models, to identify unnecessary code with respect to *each* workload.

Table 1 shows the details of the workloads. For the ML models, we choose three models of different sizes: A small model, MobileNetV2 (Sandler et al., 2018), which is a computer vision model of 4.3M parameters; A medium model, Transformer (Vaswani, 2017), which is a natu-

Table 1. Details of evaluated ML frameworks and ML workloads.

Model	Framework	Operation	DataSet	Batch Size	Epochs
MobileNetV2	PyTorch:2.3.1	Train	CIFAR10 (Krizhevsky et al., 2009) Train Set	16	3
		Inference	CIFAR10 Test Set <sup>1</sup>	4	-
	TensorFlow:2.16.2	Train	CIFAR10 Train Set	16	3
		Inference	CIFAR10 Test Set <sup>1</sup>	4	-
Transformer	PyTorch:2.3.1	Train	Multi30k (Elliott et al., 2016) Train Set	128	3
		Inference	Multi30k Test Set <sup>1</sup>	32	-
	TensorFlow:2.16.2	Train	WMT14 (Bojar et al., 2014) Train Set	128	1
		Inference	WMT14 Test Set <sup>1</sup>	32	-
Llama2	vLLM:0.6.3	Inference	Manual Input	1	-
	Transformers:4.42.3	Inference	Manual Input	1	-

<sup>1</sup> Only one batch from test set is used.

ral language processing model of 65M parameters; And a large model, Llama-2-7b-chat-hf (LLama2 for brevity) (Touvron et al., 2023a), which is a large language model of 7B parameters. In total, 10 workloads were executed using the four ML frameworks. We did not train the models to convergence, as our primary goal is to evaluate the bloat in the frameworks rather than fully train the models. Since training mainly involves repeated iterations, training a few epochs is sufficient to obtain representative results.

All the workloads in Table 1 were run on an AWS instance with 16 CPUs, 64 GB of memory, and an NVIDIA T4 GPU. For the vLLM and Transformers frameworks, we also evaluate nine more LLM models using 8×A100 GPUs, to further evaluate the bloat in a different hardware setup.

## 5.1 Overview of Bloat in ML Frameworks

We execute the workloads listed in Table 1 running NegativeML to debloat the shared libraries used by the workloads. After debloating, we re-run the workloads using the debloated shared libraries to ensure that the workloads run correctly. The removed code is considered bloat as they are not necessary for the workloads. We then compare the total file sizes of the shared libraries before and after debloating to assess file size reductions. Moreover, for host code, we compare both code size and the number of functions before and after debloating. For device code, we also analyze code size reductions and the number of elements removed. The results are presented in Table 2.

For the small model MobileNetV2, training with PyTorch involves 113 shared libraries, totaling 3762 MB. After debloating, the total file size decreases by 55%. Notably, the host code size is reduced by 68%, with 93% of functions removed. The device code size decreases by 75%, with 98% of elements removed. The device code also accounts

for the majority of the total file size and file size reduction. Inference MobileNetV2 with PyTorch shows similar reductions.

For the same MobileNetV2 model, TensorFlow uses more shared libraries compared to PyTorch, with 253 libraries for training and 251 for inference. The total file sizes and reductions are smaller than PyTorch. The host code in TensorFlow presents interesting results: it has a larger size and a greater number of functions than PyTorch, yet the reduction is less significant, indicating that TensorFlow uses more host code and functions than PyTorch. Given the fact that PyTorch can train(inference) the same model with less host code and functions, this suggests there may be unnecessary function calls within TensorFlow’s host code—functions that are used but do not contribute meaningfully to the target ML workload. The device code in TensorFlow also shows a significant reduction in size and elements, with over 99% of elements removed.

For the medium model, Transformer, both PyTorch and TensorFlow show similar results to MobileNetV2, indicating that different models do not significantly affect the bloat in the ML frameworks. For the large model, LLama2, the frameworks vLLM and Transformers were used for inference, and despite differences in frameworks, the reductions in file size, host code and device code remain significant.

The size of device code is considerably larger than that of host code for all ML frameworks. Device code also exhibits a higher reduction in both size and element count for all ML frameworks. In particular, the element count reduction in device code exceeds 97% across all workloads, underscoring that device code is significantly more bloated than host code.

Table 2. Total file size, host code, device code and their reductions of all shared libraries in each ML framework. The table shows the original value of a metric and the reduction in percentage of the metric in parentheses. K=1,000.

Model	Framework	Operation	#Lib.	Total File Size/MB	Host Code		Device Code	
					Size/MB	#Functions	Size/MB	#Elements
MobileNetV2	PyTorch	Train	113	3,762 (55)	557 (68)	616K (93)	2,279 (75)	14,062 (98)
		Inference	111	3,569 (55)	545 (70)	616K (93)	2,103 (75)	12,035 (98)
	TensorFlow	Train	253	3,274 (48)	598 (46)	984K (65)	1,774 (73)	15,081 (99)
		Inference	251	3,087 (47)	586 (48)	984K (65)	1,603 (72)	13,056 (99)
Transformer	PyTorch	Train	154	2,901 (53)	547 (71)	615K (93)	1,592 (72)	7,165 (97)
		Inference	154	2,901 (53)	547 (71)	615K (93)	1,592 (73)	7,165 (98)
	TensorFlow	Train	398	2,727 (42)	696 (46)	1,043K (66)	1,184 (70)	8,478 (98)
		Inference	396	2,640 (40)	692 (47)	1,042K (67)	1,103 (66)	8,325 (97)
LLama2	vLLM	Inference	170	3,884 (48)	724 (68)	873K (93)	1,901 (72)	7,690 (97)
	Transformers	Inference	98	2,860 (53)	511 (72)	582K (92)	1,592 (71)	7,165 (97)

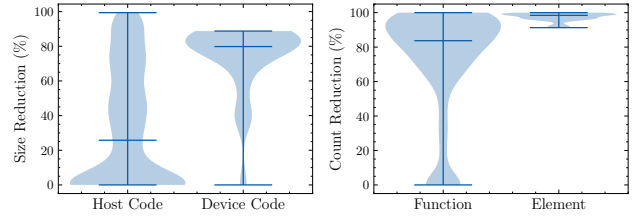
**SUMMARY.** All ML frameworks show substantial reductions in both host code ( $\geq 46\%$ ) and device code ( $\geq 66\%$ ). Device code is notably more bloated than host code, contributing to the majority of the bloat within the ML frameworks.

## 5.2 Shared Library Level Analysis

In this section, we delve deeper into the distribution of bloat within host and device code at the shared library level. For each shared library used in the workloads, we calculate the host code size reduction and function count reduction in percentage. Similarly, for each shared library, we calculate the reduction percentage in device code size and element count as well. If a shared library does not have device code, we exclude it from the device code analysis.

Figure 5a illustrates the distribution of size reduction in host and device code. The distribution patterns of host and device code show distinct differences. The median reduction for host code size is approximately 25%, with many shared libraries showing a reduction from 0% to 10%. In contrast, the median reduction for device code size is almost 80%, significantly higher than that for host code, and its distribution is also more concentrated. Figure 5b depicts the distribution of reductions in function and element counts. Notably, all shared libraries exhibit an element reduction of over 80%. The concentrated distributions for device code size and element count reductions highlight that device code is considerably more bloated than host code in all shared libraries.

For each workload, we sorted the shared libraries by their absolute file size reductions in descending order. We found that the top 10% shared libraries contribute over 90% of the total size reduction for all ML frameworks. Reductions in host code size and device code size also follow a similar pattern. For instance, as illustrated in Figure 6, the Pareto



(a) Distribution of host code size (b) Distribution of host function reduction and device code size count reduction and device element count reduction.

chart for the PyTorch Training MobileNetV2 workload shows that among 113 shared libraries, the top 8 libraries account for 90% of the total file size reduction. This result suggests that bloat follows a Power Law distribution, with a few shared libraries containing the majority of the bloat.

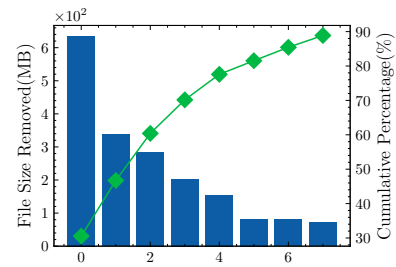


Figure 6. Pareto chart of file size reduced in the shared libraries used by the PyTorch Training MobileNetV2 workload. The names of shared libraries are shown as indices in x-axis for brevity.

**SUMMARY.** 50% of shared libraries in ML frameworks have device code reductions more than 80%. 10% of shared libraries contribute over 90% of the total size reduction.

### 5.3 Function and Element Level Analysis

To deepen the analysis, Table 3 presents reductions for the largest shared library used in each workload. All the four ML frameworks running different models use the common two shared libraries, `torch_cuda.so` and `tensorflow_cc.so`. These two libraries, which provide the core functionalities of the ML frameworks, also exhibit significant reductions in file size, device code, and host code. For the `torch_cuda.so`, the reduction in file size, host code size, and device code size are 76%, 91% and 82%, respectively. The host code in `tensorflow_cc.so` also presents the interesting results as we have discussed in §5.1: it has a much larger host code size and a greater number of functions than `torch_cuda.so`, yet the reduction is smaller. But the reductions in host code for `tensorflow_cc.so` is as significant as `torch_cuda.so`.

In the table, `torch_cuda.so` is used by three ML frameworks, PyTorch, vLLM, and Transformers, involving 6 workloads. We collect the functions used by each workload in `torch_cuda.so` to compare their similarity. Since vLLM uses a different version of `torch_cuda.so`, we exclude it from the analysis. Therefore, in total we collect five sets of functions used by five different workloads. For each pair of the function sets, we calculate their Jaccard Similarity according to the following formula:

$$J(A, B) = \frac{|A \cap B|}{|A \cup B|} \quad (1)$$

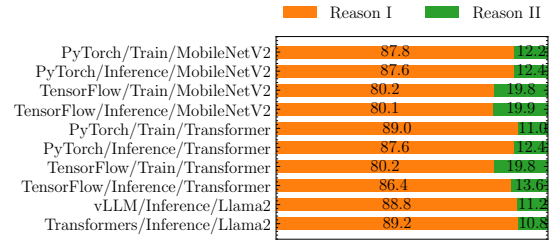
where  $A$  and  $B$  are two sets of functions used by two workloads. The Jaccard Similarity is 1 if the two sets are the same, and 0 if the two sets are disjoint. The Jaccard Similarity is also calculated for the kernels used by the five workloads. The results are shown in Table 4. We also did the same analysis for `tensorflow_cc.so`, and the results are similar and shown in the appendix.

The bottom left part of Table 4 shows the similarity of kernels between each pair of workloads. The similarity is quite low, indicating that the kernels used by different workloads are quite different. However, the similarity of functions between each pair of workloads is very high, as shown in the upper right part of Table 4. All pairs have a similarity above 0.7, indicating different workloads used many common functions, even if the workloads run with different models and frameworks. Given the fact that less than 10% of functions are actually used in the `torch_cuda.so` library in each of the five workloads, this suggests that a small subset of functions is sufficient to run various workloads.

We also examine the reasons for removed elements in device code. Negativa-ML removes an element due to one of the following two reasons: **Reason I**: The element does not match the GPU architecture; **Reason II**: The element

matches the GPU architecture, but it does not have any used kernels. We identify the reason for each removed element.

Figure 7 shows that for all workloads, over 80% of removed elements are due to Reason I, i.e., the element does not match the GPU architecture. The cause of these unmatched elements is that the device code in these shared libraries are built to support various GPU architectures, leading to numerous unnecessary elements for workloads on a specific GPU. For example, in our experiment, we observed a single shared library in the PyTorch framework contained elements for 6 different GPU architectures. If the library is deployed on a specific GPU architecture, the elements for the five other architectures are unnecessary. This reveals a deep reason for bloat: software bloat can stem from hardware.



**SUMMARY.** Different workloads used a lot of common functions in the core shared libraries. Most elements removed in device code are due to the mismatch of GPU architecture.

### 5.4 Runtime Performance Analysis

In this section, we evaluate runtime performance improvements after debloating. Initially, each workload is executed ten times using the original shared libraries. Then, based on the previous finding that a few shared libraries contribute the majority of bloat, we replace the top 8 largest shared libraries with their debloated versions and re-ran the workloads ten times. We then compare the average runtime performance between the two runs. Table 5 summarizes the average runtime performance improvements achieved with the debloated shared libraries.

Running workloads with debloated libraries reduce memory usage (both host and GPU) and execution time. The best improvement is observed in the PyTorch Inference MobileNetV2 workload, with reductions of 74.6% in peak host memory, 69.6% in peak GPU memory, and 44.6% in execution time. Inference workloads generally show better improvement than training workloads. Across all workloads, average absolute reductions are 2501 MB for peak host memory, 443 MB for peak GPU memory, and 2.6 seconds for execution time. Notably, the absolute execution time reduction remains relatively constant, regardless of the actual execution duration. This improvement stems from



Table 3. Static size, function count and element count of the core shared libraries in ML frameworks. The table shows the original value of a metric and the reduction in percentage of the metric in parentheses. K=1000.

Model	Framework	Operation	Lib. Name	File Size/MB	Host Code		Device Code	
					Size/MB	#Functions	Size/MB	#Elements
MobileNetV2	PyTorch	Train	torch_cuda.so	841 (76)	42 (91)	78K (93)	729 (82)	2,324 (98)
		Inference	torch_cuda.so	841 (76)	42 (92)	78K (93)	729 (82)	2,324 (98)
	TensorFlow	Train	tensorflow.cc.so	965 (43)	300 (59)	670K (51)	298 (79)	1,637 (100)*
		Inference	tensorflow.cc.so	965 (43)	300 (61)	670K (52)	298 (79)	1,637 (100)*
Transformer	PyTorch	Train	torch_cuda.so	841 (73)	42 (91)	78K (93)	729 (79)	2,324 (96)
		Inference	torch_cuda.so	841 (76)	42 (92)	78K (94)	729 (82)	2,324 (98)
	TensorFlow	Train	tensorflow.cc.so	965 (43)	300 (59)	670K (51)	298 (79)	1,637 (100)*
		Inference	tensorflow.cc.so	965 (41)	300 (59)	670K (52)	298 (73)	1,637 (94)
LLama2	vLLM	Inference	torch_cuda.so	861 (74)	43 (91)	78K (93)	747 (80)	2,359 (97)
	Transformers	Inference	torch_cuda.so	841 (73)	42 (91)	78K (93)	729 (79)	2,324 (96)

\* The reduction is 99.8% and rounded to 100%.

Table 4. Jaccard Similarity of used functions and kernels in torch\_cuda.so for each pair of workloads. The bottom left shows the similarity of kernels between each pair of workloads. The top right shows the similarity of functions between each pair of workloads.

			MobileNetV2 PyTorch		Transformer PyTorch		LLama2 Transformers
			Train	Inference	Train	Inference	Inference
MobileNetV2	PyTorch	Train	-	0.96	0.89	0.89	0.73
		Inference	0.42	-	0.89	0.92	0.74
Transformer	PyTorch	Train	0.12	0.06	-	0.94	0.75
		Inference	0.06	0.13	0.24	-	0.77
LLama2	Transformers	Inference	0.07	0.08	0.07	0.08	-

reduced code size, which decreases the time required to load the code into memory. This execution time improvement is especially impactful for tasks sensitive to cold start latency, such as serverless ML applications.

**SUMMARY.** Debloating shared libraries significantly reduces both host and GPU memory usage. The time required to load the code into memory is also reduced, leading to shorter execution times.

## 5.5 Evaluation on Distributed Inference

In this section, we present debloating results for additional ML workloads, focusing on two LLM inference frameworks, vLLM and Transformers. We select the top 9 LLMs from the Hugging Face Open LLM Leaderboard (Beeching et al., 2023) and deploy them on both frameworks using distributed inference with 8xA100 40GB GPUs. This setup aims to evaluate whether debloating works with distributed inference under a different hardware setup. Results are detailed in Table 7 in the Appendix.

The debloating results of distributed inference with 8 GPUs are still as significant as those of single-GPU inference. For inference with 8 GPUs, vLLM uses slightly fewer shared li-

braries than the results of a single GPU, while Transformers uses nearly the same number of libraries. The reductions in file size, host code size, function count, and device code size align closely with the results using a single GPU. However, the element count reduction in device code is lower than that of single-GPU inference, suggesting that distributed inference utilizes more kernels in device code. Additionally, the reduction metrics are similar across different models, once again indicating that different models do not significantly affect the bloat in the ML frameworks.

**SUMMARY.** Debloating results of vLLM and Transformers using distributed inference on 8 GPUs are consistent with those of single-GPU inference.

## 5.6 Kernel Detector Performance Overhead

To assess the performance overhead introduced by the kernel detector on the target ML workload, we first run the PyTorch Training MobileNetV2 workload 10 times and recorded the average execution time. Next, we ran the same workload, this time with tracing enabled by the kernel detector and by NSys respectively, each for 10 runs. We then compare the average execution times across the three setups.

Table 5. Average runtime performance using original shared libraries and reductions using debloated shared libraries. The numbers in parentheses are the percentage of reduction. The standard deviation of all metrics for each workload is less than 2% and is not shown.

Model	Framework	Operation	Peak Host Memory/MB	Peak GPU Memory/MB	Execution Time/s
MobileNetV2	PyTorch	Train	5,487 (64.2)	1,539 (48.1)	179 (2.3)
		Inference	4,943 (74.6)	972 (69.6)	8 (44.6)
	TensorFlow	Train	6,009 (48.7)	14,395 (2.8)	53 (5.5)
		Inference	4,850 (60.0)	14,323 (2.8)	12 (24.2)
Transformer	PyTorch	Train	4,151 (56.0)	9,381 (5.0)	200 (1.1)
		Inference	4,054 (65.8)	1,349 (42.3)	13 (20.3)
	TensorFlow	Train	15,652 (13.6)	14,149 (1.6)	4,779 (0.0)
		Inference	4,217 (36.5)	14,069 (1.3)	69 (1.8)
Llama2	vLLM	Inference	12,527 (11.8)	14,679 (2.1)	43 (12.7)
	Transformers	Inference	12,065 (10.4)	13,793 (3.2)	21 (8.9)
Average Absolute Reduction $\pm\sigma$			2501 $\pm$ 825	443 $\pm$ 171	2.6 $\pm$ 1.6

The average execution time for the original workload was 180 seconds. With the kernel detector enabled, the execution time increased to 253 seconds, a 41% overhead. In contrast, tracing with NSys increases the execution time to 407 seconds, introducing a 126% overhead. The kernel detector imposes significantly lower overhead than NSys, making it a more practical choice for detecting used kernels, especially for long-running workloads like ML training. We note that this is a one time overhead that can occur in, e.g., a profiling stage before the actual deployment.

## 6 DISCUSSION

As Sculley et al. (Sculley et al., 2015) highlight, ML systems have hidden technical debt due to a set of ML-specific issues. Our work emphasizes this technical debt by exposing the hidden bloat in ML frameworks. Software bloat has been a long-standing issue in the software industry. While existing debloating research has focused on traditional software, bloat in ML systems is not well understood. The uniqueness of ML systems is that they contain both host and device code, leading to significant bloat. Our evaluations over four ML frameworks across ten workloads with around 300 shared libraries show significant bloat in these frameworks, with up to 72% size reduction in host code and 75% size reduction in device code. Furthermore, unlike traditional software, ML frameworks experience substantial bloat in device code. All this bloat leads to increased storage needs, higher memory usage, and longer execution times.

In our evaluations, only a small subset of code is consistently utilized. This suggests that code unused by one workload is likely unnecessary for others as well. Besides, existing research focuses solely on unused code, overlooking “used bloat” — code executed by a workload but not contributing meaningfully to the performance or functionality. For instance, when training a model with a specific optimizer, the optimizer may initialize a context with numerous non-

essential function calls. Compared with PyTorch, the larger host code size but smaller reduction in TensorFlow may indicate the presence of “used bloat”. Such “used bloat” is particularly harmful, as it is executed and thus consumes scarce memory, CPU, and GPU resources. Moreover, it is more difficult to detect as it is actually executed. Future research could focus on identifying and eliminating this “used bloat”.

Shared libraries in ML frameworks are significantly larger than traditional shared libraries (Zhang et al., 2024), mainly due to device code as shown in this work. As storage and network bandwidth are critical bottlenecks in edge data centers (Richins et al., 2021), the file size reduction achieved by debloating can help alleviate these bottlenecks.

## 7 CONCLUSION

We propose a novel approach to debloat ML frameworks by removing unnecessary code in both host and device code within shared libraries. Our approach first detects kernel names used in device code by running ML workloads, such as training or inference a model. We then locate the used kernels within the shared libraries and remove the unused code. We implement our approach based on an existing debloating tool, and evaluate it on four ML frameworks across ten workloads over 300 shared libraries. Our evaluation shows that ML frameworks are highly bloated, with up to 55% size reduction in shared libraries in these frameworks. We show that up to 75% of device code and 99% of device elements being unnecessary for target ML workloads; Up to 72% of host code and 93% of host functions are unnecessary for target ML workloads. This bloat not only increases storage overhead but also degrades runtime performance. Debloating these frameworks reduces the peak memory usage, peak GPU memory usage, and startup time by up to 74.6%, 69.6%, and 44.6%, respectively.

## REFERENCES

- Text Generation Inference — huggingface.co. <https://huggingface.co/docs/text-generation-inference/index>. [Accessed 28-10-2024].
- CUDA Binary Utilities — docs.nvidia.com. <https://docs.nvidia.com/cuda/cuda-binary-utilities/index.html>, a. [Accessed 28-10-2024].
- CUDA Deep Neural Network — developer.nvidia.com. <https://developer.nvidia.com/cudnn>, b. [Accessed 28-10-2024].
- cuBLAS — developer.nvidia.com. <https://developer.nvidia.com/cublas>, c. [Accessed 28-10-2024].
- NVIDIA CUDA Profiling Tools Interface (CUPTI) - CUDA Toolkit — developer.nvidia.com. <https://developer.nvidia.com/cupti>, d. [Accessed 28-10-2024].
- NVIDIA CUDA Compiler Driver — docs.nvidia.com. <https://docs.nvidia.com/cuda/cuda-compiler-driver-nvcc/index.html#using-separate-compilation-in-cuda>, e. [Accessed 27-10-2024].
- NVIDIA Nsight Systems — developer.nvidia.com. <https://developer.nvidia.com/nsight-systems>, f. [Accessed 28-10-2024].
- File Format (Linker and Libraries Guide) — docs.oracle.com. <https://docs.oracle.com/cd/E19683-01/816-1386/6m7qcoblj/index.html>. [Accessed 28-10-2024].
- Abadi, M., Barham, P., Chen, J., Chen, Z., Davis, A., Dean, J., Devin, M., Ghemawat, S., Irving, G., Isard, M., et al. {TensorFlow}: a system for {Large-Scale} machine learning. In *12th USENIX symposium on operating systems design and implementation (OSDI 16)*, pp. 265–283, 2016.
- Agadakos, I., Jin, D., Williams-King, D., Kemerlis, V. P., and Portokalidis, G. Nibbler: debloating binary shared libraries. In *Proceedings of the 35th Annual Computer Security Applications Conference*, pp. 70–83, 2019.
- Ahmad, A. A., Noor, A. R., Sharif, H., Hameed, U., Asif, S., Anwar, M., Gehani, A., Zaffar, F., and Siddiqui, J. H. Trimmer: an automated system for configuration-based software debloating. *IEEE Transactions on Software Engineering*, 48(9):3485–3505, 2021.
- anonymous. Reference anaomized for double blind.
- Azad, B. A., Laperdrix, P., and Nikiforakis, N. Less is more: Quantifying the security benefits of debloating web applications. In *28th USENIX Security Symposium (USENIX Security 19)*, pp. 1697–1714, 2019.
- Beeching, E., Fourrier, C., Habib, N., Han, S., Lambert, N., Rajani, N., Sanseviero, O., Tunstall, L., and Wolf, T. Open llm leaderboard (2023-2024). [https://huggingface.co/spaces/open-llm-leaderboard/open\\_llm\\_leaderboard](https://huggingface.co/spaces/open-llm-leaderboard/open_llm_leaderboard), 2023.
- Bhardwaj, R., Nambiar, A. R., and Dutta, D. A study of machine learning in healthcare. In *2017 IEEE 41st annual computer software and applications conference (COMPSAC)*, volume 2, pp. 236–241. IEEE, 2017.
- Biswas, P., Burow, N., and Payer, M. Code specialization through dynamic feature observation. In *Proceedings of the Eleventh ACM Conference on Data and Application Security and Privacy*, pp. 257–268, 2021.
- Bojar, O., Buck, C., Federmann, C., Haddow, B., Koehn, P., Leveling, J., Monz, C., Pecina, P., Post, M., Saint-Amand, H., Soricut, R., Specia, L., and Tamchyna, A. s. Findings of the 2014 workshop on statistical machine translation. In *Proceedings of the Ninth Workshop on Statistical Machine Translation*, pp. 12–58, Baltimore, Maryland, USA, June 2014. Association for Computational Linguistics. URL <http://www.aclweb.org/anthology/W/W14/W14-3302>.
- Brown, M. D. and Pande, S. Carve: Practical security-focused software debloating using simple feature set mappings. In *Proceedings of the 3rd ACM Workshop on Forming an Ecosystem Around Software Transformation*, pp. 1–7, 2019.
- Brown, M. D., Meily, A., Fairservice, B., Sood, A., Dorn, J., Kilmer, E., and Eytchison, R. A broad comparative evaluation of software debloating tools. pp. 3927–3943, 2024.
- Contributors, L. Lmdeploy: A toolkit for compressing, deploying, and serving llm. <https://github.com/InternLM/lmdeploy>, 2023.
- Elliott, D., Frank, S., Sima'an, K., and Specia, L. Multi30k: Multilingual english-german image descriptions. In *Proceedings of the 5th Workshop on Vision and Language*, pp. 70–74. Association for Computational Linguistics, 2016. doi: 10.18653/v1/W16-3210. URL <http://www.aclweb.org/anthology/W16-3210>.
- Fernandez, J., Kahn, J., Na, C., Bisk, Y., and Strubell, E. The framework tax: Disparities between inference efficiency in nlp research and deployment. *arXiv preprint arXiv:2302.06117*, 2023.

- Jiang, X., Wang, H., Chen, Y., Wu, Z., Wang, L., Zou, B., Yang, Y., Cui, Z., Cai, Y., Yu, T., et al. Mnn: A universal and efficient inference engine. *Proceedings of Machine Learning and Systems*, 2:1–13, 2020.
- Ko, H., Lee, S., Park, Y., and Choi, A. A survey of recommendation systems: recommendation models, techniques, and application fields. *Electronics*, 11(1):141, 2022.
- Krizhevsky, A., Hinton, G., et al. Learning multiple layers of features from tiny images. 2009.
- Kuo, H.-C., Chen, J., Mohan, S., and Xu, T. Set the configuration for the heart of the os: On the practicality of operating system kernel debloating. *Proceedings of the ACM on Measurement and Analysis of Computing Systems*, 4(1):1–27, 2020.
- Kwon, W., Li, Z., Zhuang, S., Sheng, Y., Zheng, L., Yu, C. H., Gonzalez, J. E., Zhang, H., and Stoica, I. Efficient memory management for large language model serving with pagedattention. In *Proceedings of the ACM SIGOPS 29th Symposium on Operating Systems Principles*, 2023.
- Navas, J. A. and Gehani, A. Occam-v2: combining static and dynamic analysis for effective and efficient whole-program specialization. *Communications of the ACM*, 66(4):40–47, 2023.
- OpenAI, Achiam, J., Adler, S., Agarwal, S., Ahmad, L., Akkaya, I., Aleman, F. L., Almeida, D., Altenschmidt, J., Altman, S., Anadkat, S., Avila, R., Babuschkin, I., Balaji, S., Balcom, V., Baltescu, P., Bao, H., Bavarian, M., Belgum, J., Bello, I., Berdine, J., Bernadett-Shapiro, G., Berner, C., Bogdonoff, L., Boiko, O., Boyd, M., Brakman, A.-L., Brockman, G., Brooks, T., Brundage, M., Button, K., Cai, T., Campbell, R., Cann, A., Carey, B., Carlson, C., Carmichael, R., Chan, B., Chang, C., Chantzis, F., Chen, D., Chen, S., Chen, R., Chen, J., Chen, M., Chess, B., Cho, C., Chu, C., Chung, H. W., Cummings, D., Currier, J., Dai, Y., Decareaux, C., Degry, T., Deutsch, N., Deville, D., Dhar, A., Dohan, D., Dowling, S., Dunning, S., Ecoffet, A., Eleti, A., Eloundou, T., Farhi, D., Fedus, L., Felix, N., Fishman, S. P., Forte, J., Fulford, I., Gao, L., Georges, E., Gibson, C., Goel, V., Gogineni, T., Goh, G., Gontijo-Lopes, R., Gordon, J., Grafstein, M., Gray, S., Greene, R., Gross, J., Gu, S. S., Guo, Y., Hallacy, C., Han, J., Harris, J., He, Y., Heaton, M., Heidecke, J., Hesse, C., Hickey, A., Hickey, W., Hoeschele, P., Houghton, B., Hsu, K., Hu, S., Hu, X., Huizinga, J., Jain, S., Jain, S., Jang, J., Jiang, A., Jiang, R., Jin, H., Jin, D., Jomoto, S., Jonn, B., Jun, H., Kaftan, T., Łukasz Kaiser, Kamali, A., Kanitscheider, I., Keskar, N. S., Khan, T., Kilpatrick, L., Kim, J. W., Kim, C., Kim, Y., Kirchner, J. H., Kiros, J., Knight, M., Kokotajlo, D., Łukasz Kondraciuk, Kondrich, A., Konstantinidis, A., Kopic, K., Krueger, G., Kuo, V., Lampe, M., Lan, I., Lee, T., Leike, J., Leung, J., Levy, D., Li, C. M., Lim, R., Lin, M., Lin, S., Litwin, M., Lopez, T., Lowe, R., Lue, P., Makanju, A., Malfacini, K., Manning, S., Markov, T., Markovski, Y., Martin, B., Mayer, K., Mayne, A., McGrew, B., McKinney, S. M., McLeavey, C., McMillan, P., McNeil, J., Medina, D., Mehta, A., Menick, J., Metz, L., Mishchenko, A., Mishkin, P., Monaco, V., Morikawa, E., Mossing, D., Mu, T., Murati, M., Murk, O., Mély, D., Nair, A., Nakano, R., Nayak, R., Neelakantan, A., Ngo, R., Noh, H., Ouyang, L., O’Keefe, C., Pachocki, J., Paino, A., Palermo, J., Pantuliano, A., Parascandolo, G., Parish, J., Parparita, E., Passos, A., Pavlov, M., Peng, A., Perelman, A., de Avila Belbute Peres, F., Petrov, M., de Oliveira Pinto, H. P., Michael, Pokorný, Pokrass, M., Pong, V. H., Powell, T., Power, A., Power, B., Proehl, E., Puri, R., Radford, A., Rae, J., Ramesh, A., Raymond, C., Real, F., Rimbach, K., Ross, C., Rotsted, B., Roussez, H., Ryder, N., Saltarelli, M., Sanders, T., Santurkar, S., Sastry, G., Schmidt, H., Schnurr, D., Schulman, J., Selsam, D., Sheppard, K., Sherbakov, T., Shieh, J., Shoker, S., Shyam, P., Sidor, S., Sigler, E., Simens, M., Sitkin, J., Slama, K., Sohl, I., Sokolowsky, B., Song, Y., Staudacher, N., Such, F. P., Summers, N., Sutskever, I., Tang, J., Tezak, N., Thompson, M. B., Tillet, P., Tootoonchian, A., Tseng, E., Tuggle, P., Turley, N., Tworek, J., Uribe, J. F. C., Vallone, A., Vijayvergiya, A., Voss, C., Wainwright, C., Wang, J. J., Wang, A., Wang, B., Ward, J., Wei, J., Weinmann, C., Welihinda, A., Welinder, P., Weng, J., Weng, L., Wiethoff, M., Willner, D., Winter, C., Wolrich, S., Wong, H., Workman, L., Wu, S., Wu, J., Wu, M., Xiao, K., Xu, T., Yoo, S., Yu, K., Yuan, Q., Zaremba, W., Zellers, R., Zhang, C., Zhang, M., Zhao, S., Zheng, T., Zhuang, J., Zhuk, W., and Zoph, B. Gpt-4 technical report, 2024. URL <https://arxiv.org/abs/2303.08774>.
- Parekh, D., Poddar, N., Rajpurkar, A., Chahal, M., Kumar, N., Joshi, G. P., and Cho, W. A review on autonomous vehicles: Progress, methods and challenges. *Electronics*, 11(14):2162, 2022.
- Paszke, A., Gross, S., Massa, F., Lerer, A., Bradbury, J., Chanan, G., Killeen, T., Lin, Z., Gimelshein, N., Antiga, L., et al. Pytorch: An imperative style, high-performance deep learning library. *Advances in neural information processing systems*, 32, 2019.
- Qian, C., Hu, H., Alharthi, M., Chung, P. H., Kim, T., and Lee, W. {RAZOR}: A framework for post-deployment software debloating. In *28th USENIX security symposium (USENIX Security 19)*, pp. 1733–1750, 2019.
- Quach, A., Erinfolami, R., Demicco, D., and Prakash, A. A multi-os cross-layer study of bloating in user programs, kernel and managed execution environments. In *Proceedings of the 2017 Workshop on Forming an Ecosystem Around Software Transformation*, pp. 65–70, 2017.



- Quach, A., Prakash, A., and Yan, L. Debloating software through {Piece-Wise} compilation and loading. In *27th USENIX security symposium (USENIX Security 18)*, pp. 869–886, 2018.
- Rastogi, V., Davidson, D., De Carli, L., Jha, S., and McDaniel, P. Cimplifier: automatically debloating containers. In *Proceedings of the 2017 11th Joint Meeting on Foundations of Software Engineering*, pp. 476–486, 2017.
- Richins, D., Doshi, D., Blackmore, M., Nair, A. T., Pathapati, N., Patel, A., Daguman, B., Dobrijalowski, D., Illickal, R., Long, K., et al. Ai tax: The hidden cost of ai data center applications. *ACM Transactions on Computer Systems (TOCS)*, 37(1-4):1–32, 2021.
- Sandler, M., Howard, A., Zhu, M., Zhmoginov, A., and Chen, L.-C. Mobilenetv2: Inverted residuals and linear bottlenecks. In *Proceedings of the IEEE conference on computer vision and pattern recognition*, pp. 4510–4520, 2018.
- Sculley, D., Holt, G., Golovin, D., Davydov, E., Phillips, T., Ebner, D., Chaudhary, V., Young, M., Crespo, J.-F., and Dennison, D. Hidden technical debt in machine learning systems. *Advances in neural information processing systems*, 28, 2015.
- Sinha, M., Menon, S., and Sagar, R. Llmops: Definitions, framework and best practices. In *2024 International Conference on Electrical, Computer and Energy Technologies (ICECET)*, pp. 1–6. IEEE, 2024.
- Touvron, H., Lavril, T., Izacard, G., Martinet, X., Lachaux, M.-A., Lacroix, T., Rozière, B., Goyal, N., Hambro, E., Azhar, F., et al. Llama: Open and efficient foundation language models. *arXiv preprint arXiv:2302.13971*, 2023a.
- Touvron, H., Lavril, T., Izacard, G., Martinet, X., Lachaux, M.-A., Lacroix, T., Rozière, B., Goyal, N., Hambro, E., Azhar, F., Rodriguez, A., Joulin, A., Grave, E., and Lample, G. Llama: Open and efficient foundation language models, 2023b. URL <https://arxiv.org/abs/2302.13971>.
- Vaswani, A. Attention is all you need. *Advances in Neural Information Processing Systems*, 2017.
- Wolf, T., Debut, L., Sanh, V., Chaumond, J., Delangue, C., Moi, A., Cistac, P., Rault, T., Louf, R., Funtowicz, M., Davison, J., Shleifer, S., von Platen, P., Ma, C., Jernite, Y., Plu, J., Xu, C., Scao, T. L., Gugger, S., Drame, M., Lhoest, Q., and Rush, A. M. Transformers: State-of-the-art natural language processing. In *Proceedings of the 2020 Conference on Empirical Methods in Natural Language Processing: System Demonstrations*, pp. 38–45, Online, October 2020. Association for Computational Linguistics. URL <https://www.aclweb.org/anthology/2020.emnlp-demos.6>.
- Ye, R., Liu, L., Hu, S., Zhu, F., Yang, J., and Wang, F. Jsllim: Reducing the known vulnerabilities of javascript application by debloating. In *International Symposium on Emerging Information Security and Applications*, pp. 128–143. Springer, 2021.
- Zhang, H., Alhanahnah, M., and Ali-Eldin, A. Blafs: A bloat aware file system, 2023. URL <https://arxiv.org/abs/2305.04641>.
- Zhang, H., Alhanahnah, M., Ahmed, F. A., Fatih, D., Leitner, P., and Ali-Eldin, A. Machine learning systems are bloated and vulnerable. *Proceedings of the ACM on Measurement and Analysis of Computing Systems*, 8(1):1–30, 2024.
- Ziegler, A., Geus, J., Heinloth, B., Hönig, T., and Lohmann, D. Honey, i shrunk the elfs: Lightweight binary tailoring of shared libraries. *ACM Transactions on Embedded Computing Systems (TECS)*, 18(5s):1–23, 2019.

## A APPENDIX

Listing 1. Command line used for Nsys profiling  
`nsys profile --trace=cuda -o report`  
 {Command to run the ML workload}

Table 6. Jaccard Similarity of used functions and kernels in `tensorflow.cc.so` used each pair of workloads. The bottom left shows the similarity of kernels between each pair of workloads. The top right shows the similarity of functions between each pair of workloads.

		MobileNetV2 TensorFlow		Transformer TensorFlow	
		Train	Inference	Train	Inference
MobileNetV2	TensorFlow	Train	-	0.95	0.89
		Inference	0.5	0.86	0.82
Transformer	TensorFlow	Train	0.38	-	0.88
		Inference	0.02	0.05	-

Table 7. Debloating results of vLLM and Transformers with the top 9 LLMs using distributed inference.

Framework	Model	#Lib.	Total File Size/MB	Host Code Size/MB	#Functions	Device Code Size/MB	#Elements
vLLM	c4ai_command.r.plus	137	3,790 (54)	650 (70)	837K (93)	1,910 (84)	7,587 (85)
	internlm2_5_7b_chat	135	3,790 (54)	650 (70)	837K (93)	1,910 (84)	7,587 (85)
	llama_3_70b_instruct	135	3,790 (54)	650 (70)	837K (93)	1,910 (84)	7,587 (85)
	mixtral_8x22b_instruct	137	3,790 (54)	650 (70)	837K (93)	1,910 (84)	7,587 (85)
	phi_3_medium_4k_instruct	136	4,164 (54)	655 (71)	848K (93)	2,244 (79)	8,297 (84)
	qwen_72b_instruct	136	3,792 (54)	651 (70)	837K (93)	1,910 (84)	7,587 (85)
	qwen15_110b_chat	136	3,792 (54)	651 (70)	837K (93)	1,910 (84)	7,587 (85)
	yi_15_34b	135	3,790 (54)	650 (70)	837K (93)	1,910 (84)	7,587 (85)
	zephyr_orpo_141b_a35b	137	3,790 (54)	650 (70)	837K (93)	1,910 (84)	7,587 (85)
Transformers	c4ai_command.r.plus	94	2,866 (61)	514 (73)	590K (92)	1,592 (86)	7,165 (85)
	internlm2_5_7b_chat	94	2,866 (61)	514 (73)	591K (92)	1,592 (86)	7,165 (85)
	llama_3_70b_instruct	96	2,863 (61)	513 (73)	587K (92)	1,592 (86)	7,165 (85)
	mixtral_8x22b_instruct	98	2,866 (61)	514 (73)	591K (92)	1,592 (86)	7,165 (85)
	phi_3_medium_4k_instruct	94	2,866 (61)	514 (73)	590K (92)	1,592 (86)	7,165 (85)
	qwen_72b_instruct	97	2,866 (61)	513 (73)	588K (92)	1,592 (86)	7,165 (85)
	qwen15_110b_chat	98	2,868 (61)	514 (73)	590K (92)	1,592 (86)	7,165 (85)
	yi_15_34b	97	2,866 (61)	514 (73)	590K (92)	1,592 (86)	7,165 (85)
	zephyr_orpo_141b_a35b	97	2,866 (61)	514 (73)	590K (92)	1,592 (86)	7,165 (85)